



OPEN An innovative wearable device for sensing mechanoreceptor activation during touch

Rexhina Shyti^{1,2✉}, Pascale Nays², Roberto Vargiolu¹ & Hassan Zahouani¹

Combined studies on the biophysical properties and friction-induced vibrations measured from the fingerpad during touch have yielded promising results. Thus, the ensuing investigation focuses on the underlying mechanism of how surface's roughness affects tactile perception by analysing the finger friction-induced vibrations signals so as to identify the activation of skin mechanoreceptors. The test consists in measuring the skin friction-induced vibrations through the finger sliding against different surfaces' roughness by dint of a wearable augmented finger. The test illustrates that the magnitude of the vibration acceleration signal increases the rougher the surface is, which follows the trends observed in the scientific literature. A notable correlation was identified between amplitude and spacing parameters, validating the robustness of the measurements. To ensure data comparability, parameters such as normal force and sliding direction were meticulously controlled for each participant. Furthermore, the advanced signal processing strategy uncovered additional parameters related to the activation of skin mechanoreceptors, providing deeper insights into what can be perceived by the finger during tactile exploration. Correlations between these signal parameters and the topographical characteristics of the surfaces were explored, demonstrating that the magnitude of several parameters increased with surface roughness. These findings highlight the capabilities of the innovative device to discriminate different touch.

Keywords Fingerpad, Tactile perception, Friction-induced vibrations, Texture perception, Vibrotactile device

Human beings explore and perceive the characteristics of object surfaces through their fingers. Understanding the mechanisms of tactile perception has received significant attention over the years, both for research purposes and industrial applications. The concept of tactile perception can be explored from physiological, mechanical, and psychological perspectives¹. In fact, during tactile exploration, the motion of the finger rubbing against the surface results in vibrations induced in the skin through the fingerpad mechanical deformation^{2–4}. These vibrations generated through the three main layers of the skin will stimulate mechanoreceptors—touch sensors—embedded at various depths^{5–8}.

Four types of mechanoreceptors are responsible for touch sensation, pressure, vibrations, and cutaneous tension that result from the contact between the finger and the surface: Meissner's corpuscles, Pacinian corpuscles, Merkel's disks, and Ruffini's corpuscles⁹. Moreover, mechanoreceptors are divided into two types; slowadapting type I, II named SA-I, II; and fastadapting type I, II named FA-I, II; scattering in the skin for static (≤ 5 Hz) and dynamic (5–1000 Hz) force detecting^{9–12}. As the conveyed vibrations on the skin determine tactile sensation, consequently during touch the physiological properties of the finger (mechanical properties—elasticity, viscoelasticity, physicochemical properties—sebum, hydration) will impact tactile sensation¹³.

The skin's friction and deformation while assessing the surface texture—that is composed of its three main parameters: roughness, compliance and viscoelasticity¹⁴—is impacted by the mechanical properties of both the fingerpad and the surface. These deformations perceived by the mechanoreceptors are converted into different electrochemical signals. Finally, touch result from cellular transduction of mechanical stimuli into electrochemical signals that are then transmitted to the brain: the mechanotransduction phenomenon^{15,16}. Previous investigations have focused their interest on the characterization of finger and textured surface interaction, e.g., by measuring the friction coefficient, the vibratory level, or the contact area^{14,17–23}. However, to our knowledge none of them have tried to establish a link between the physical touch parameters that can be measured and the mechanoreceptors' activation. The vibratory level is a parameter commonly measured to investigate touch^{24–28}, yet in the light of the development of an innovative device, measuring the fingertip's skin

¹Laboratoire de tribologie et dynamique des systèmes, Ecole centrale de Lyon, Ecully, France. ²Renault Group, Technocentre Renault, Guyancourt, France. ✉email: rexhina.shyti@outlook.fr

vibrations during dynamic touch is enabled. The signals could deliver interesting data providing information about mechanoreceptors' activation, a way to connect with the psychological aspect. Thus, this method could assist in gaining a better comprehension of tactile sensation, and tactile perception through physical and objective measurement.

Previous studies have tried to ascertain correlation between data collected from the interaction with specific textured surfaces by not only mimicking the finger structure so as to create an artificial finger capable of garnering repeatable data by setting the touch condition—i.e., direction, length, velocity, normal force—but also with piezoelectric sensors to investigate vibrations. Indeed, its form often takes a layered structure composed of flexible substrates and sensory layer^{29–33}. Nonetheless, these researches have illustrated that limitations are discovered due to the materials utilized (silicon, ceramics, glass).

The wearable innovative device developed is an augmented finger utilizing the fingertip as a probe enabling the measurements of the skin's vibration. Such recordings permit the acquisition of realistic inputs of the finger/surface interaction. Employing progressive textured surfaces—characterized to obtain topographical data—can provide normalized samples that could be assessed through touch measurement. Volunteers equipped with the tactile device explore the samples through a controlled-dynamic exploration, and signal measurements are processed to extract the parameters of interest. By dint of statistical analysis to investigate relationships between the surface characteristics, finger's vibration measurement, and mechanoreceptors' activation, the device, in all likelihood, could be a tremendous tool to collect tactile perception information. Therefore, a method to obtain objective touch assessment through physical measurement during active touch is proposed.

Materials and methods

Samples

In order to reflect the difference of tactile perception, 12 samples were chosen with a progressive roughness level. The dataset stems from a single material (ABS), and the surfaces were textured utilising the identical process (laser texturing) purchased from Eschmann Textures International. Figure 1 depicts the three-dimensional (3D) topographies of this dataset's surfaces and Tables 1 and 2 provide the topographical characteristics of the surfaces. Sample VDL#12 is the smoothest and sample VDL#45 is the roughest within the samples tested in this research. A mean value of $R_a = 0,6 \mu\text{m}$, $R_z = 3,4 \mu\text{m}$ and $R_a = 16 \mu\text{m}$, $R_z = 68 \mu\text{m}$ was found for the samples VDL#12 and VDL#45, respectively. All samples have the same dimension 40 mm x 50 mm and were cleaned with a soft tissue prior to each test.

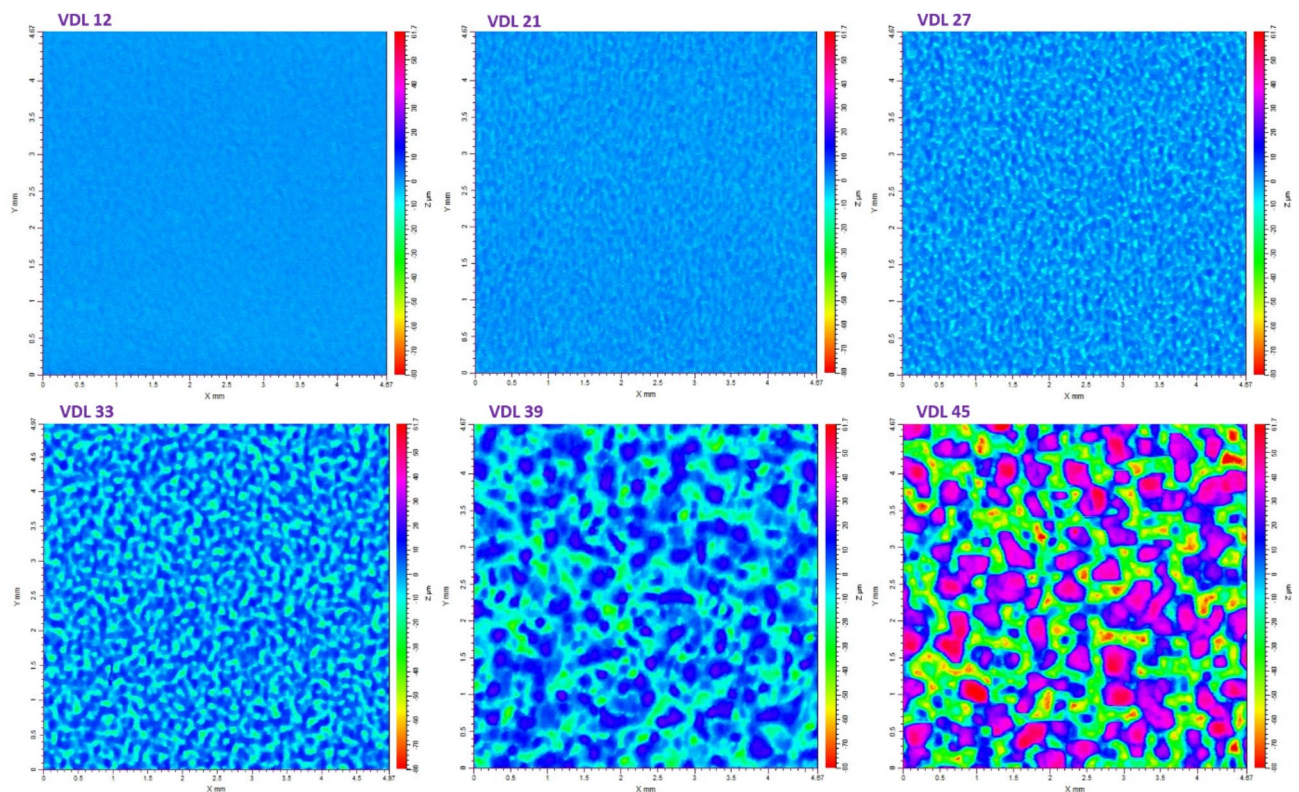


Fig. 1. Textured surface with progressive roughness, images of the samples obtained by white light scanning interferometry from the smoothest sample (VDL#12) to the roughest one (VDL #45).

Parameters	Definitions
<i>Sa</i>	Arithmetic mean height
<i>Sq</i>	Root mean square height
<i>SPt</i>	Maximum peak-pit height
<i>Sz</i>	Mean height peak-pit
<i>Spm</i>	Mean peak height
<i>Svm</i>	Mean pit height
<i>Smx</i>	Mean wavelength in x direction
<i>Smy</i>	Mean wavelength in y direction

Table 1. Definition of roughness parameters measured through the surface using a specific topographical software TopoSurf[®].

Samples	Roughness parameters							
	<i>Sa</i> (mm)	<i>Sq</i> (mm)	<i>SPt</i> (mm)	<i>Sz</i> (mm)	<i>Spm</i> (mm)	<i>Svm</i> (mm)	<i>Smx</i> (mm)	<i>Smy</i> (mm)
VLD 12	7.10 E-04	8.95 E-04	6.07 E-03	5.81 E-03	3.28 E-03	2.53 E-03	8.00 E-02	6.12 E-02
VLD 15	1.01 E-03	1.27 E-03	9.87 E-03	8.01 E-03	4.30 E-03	3.71 E-03	1.03 E-01	9.54 E-02
VLD 18	1.01 E-03	1.28 E-03	1.01 E-02	9.36 E-03	5.59 E-03	3.77 E-03	8.97 E-02	7.90 E-02
VLD 21	1.30 E-03	1.64 E-03	1.14 E-02	1.11 E-02	5.23 E-03	5.92 E-03	1.00 E-01	1.01 E-01
VLD 24	1.89 E-03	2.37 E-03	1.60 E-02	1.58 E-02	7.02 E-03	8.75 E-03	1.17 E-01	1.16 E-01
VLD 27	2.56 E-03	3.25 E-03	1.99 E-02	1.98 E-02	7.29 E-03	1.25 E-02	1.36 E-01	1.44 E-01
VLD 30	4.37 E-03	5.25 E-03	2.66 E-02	2.59 E-02	1.05 E-02	1.54 E-02	1.97 E-01	1.99 E-01
VLD 33	6.22 E-03	7.52 E-03	3.61 E-02	3.59 E-02	1.31 E-02	2.28 E-02	2.19 E-01	2.22 E-01
VLD 36	8.74 E-03	1.10 E-02	6.99 E-02	5.61 E-02	2.30 E-02	3.31 E-02	2.84 E-01	2.76 E-01
VLD 39	9.18 E-03	1.12 E-02	6.36 E-02	5.98 E-02	2.30 E-02	3.67 E-02	3.60 E-01	3.71 E-01
VLD 42	2.04 E-02	2.46 E-02	1.26 E-01	1.16 E-01	4.32 E-02	7.30 E-02	4.30 E-01	4.36 E-01
VLD 45	2.67 E-02	3.09 E-02	1.45 E-01	1.28 E-01	5.34 E-02	7.45 E-02	5.54 E-01	5.10 E-01

Table 2. Textured surfaces characterized by white light scanning interferometer. Roughness parameters measured through the surface using a specific topographical software TopoSurf[®].

Participants

Ten participants aged between 23 and 34 years (average age of 26 years old) volunteered and were recruited for the investigation. To reduce any differences related to age, the participants were all young with an equitable gender balance respected (5 males and 5 females). The volunteers came from diverse backgrounds and were not exclusively students. All participants were trained to use the device, they volunteered and signed a statement that they have no physical problems or mental disorders which might influence the results of the tests. The investigation conformed to the principles of the Declaration of Helsinki and the experiment was performed in accordance with relevant guidelines and regulations. All participants gave informed consent. The measurements were performed in situ and were non-invasive, nor harmless and involved only the fingertip thus no ethical approval was necessary for this study. Prior to each measurement, volunteers were asked to wash their hands with soap and gently dry their fingers with a soft towel. During the experiments, the order of the samples for all the participants was assigned randomly, thus the results are not influenced by the running order. All data were statistically analysed by using JMP 17.0.0 (student license) with significance set as 0.05.

Haptic device

An in-house developed setup was employed to conduct the tribological test of the finger-surface contact, as shown in Fig. 2 Touchy Finger[®] is an augmented finger that records and measures the vibratory level (*La* in dB) and normal force (*F_N* in mN) during a gliding contact between the fingertip and the surface. By dint of an accelerometer (sampling rate of 3.2 kHz) and an effort gauge (ref. 02XSR-36 S, JST) located in the device's tip, the wristband box collects the data, and the dedicated software provides two distinct signals describing the finger force and the vibration signal respectively. In addition, the device comes with different ring sizes adaptable to the finger size of each participant. The device has been developed to replace subjective data from touch with physical parameters. The technological innovation Touchy Finger[®] permits the acquisition of various physical parameters labelling the finger's mechanical response due to contact with any type of surface. Prior to accessing the contact information the vibratory signal may contain, it ought to be pre-processed and analysed both in time and in the frequency domain. The data measurement and parameters calculation are then fit together in order to extract interesting correlations.

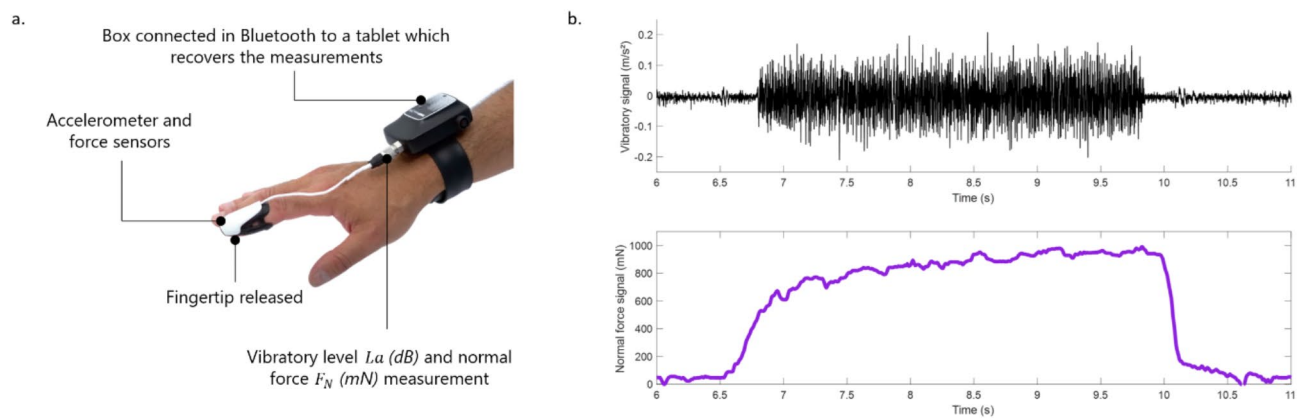


Fig. 2. Tribo-haptic device measuring the fingerpad vibrations during tactile exploration. (a) Touchy finger® device measuring the skin vibrations and normal force applied during dynamic touch (b) Vibratory signal and normal force signal measured with Touchy Finger® during one sliding motion.

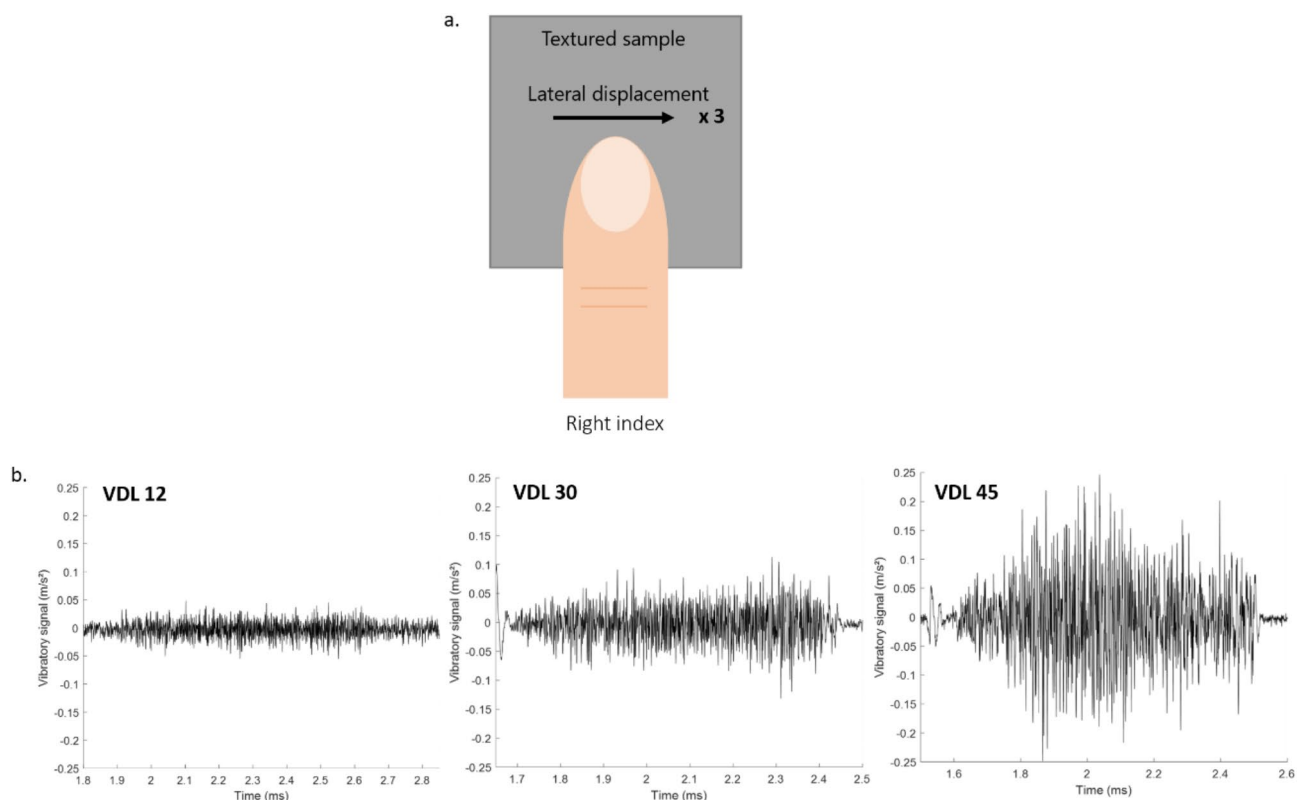


Fig. 3. Measurement protocol of the samples. (a) Touch gesture, lateral displacement of the participant's right finger (b) Vibratory signal measured with the Touchy Finger® device, three signals extracted out of the twelve samples investigated in the study.

Experiments

The device captures both the normal force signal and the accelerometer signal. The experiments were achieved at the laboratory and all tests were conducted at the same ambient temperature of approximately 21 °C and a relative humidity of 45–50%. Furthermore, during the tests, the samples were fixed on the table to avoid any vibrations related to its movement.

The purpose of the study is to characterize a natural dynamic touch, thus, equipped with Touchy Finger®, the participant's hand was not constrained. However, so as to obtain repeatable and reproducible measurement they were asked to rub their finger on the surface sample translating it on a 5 cm length from left to right Fig. 3, to apply an equivalent normal force of 400 mN, and move the finger at an approximative 3 cm/s. These parameters were selected based on findings from the literature, as they closely mimic the natural tactile exploration of surfaces

by the human finger. For each participant, measurements were performed nine times per sample (3 repetitions of 3 finger/surface contacts). 12 samples fabricated by direct laser surface texturing were assessed using the protocol defined earlier. The subjects were requested to utilize the index of their dominant hand (all subjects were right-handed) to touch and slide along the sample surface from the left to the right side. The same sliding condition and direction were performed during the physical measurements. According to previous studies^{14,32}, the force, the sliding direction to the texture and velocity can alter or enhance the dynamic tactile friction due to the fingertip's deformation. Measuring the force applied, made possible by the device, provided us with a straightforward method to validate our data. Additionally, through signal processing, we were able to determine the velocity of the fingertip's movement, enabling us to verify the touch conditions for each volunteer and each measurement. Measurements that did not meet the specified criteria (400 mN force and 3 cm/s velocity) were excluded from the study. The fingertip is completely exposed, and the design of the device allows for free hand movement, ensuring there is no restriction or interference during touch that could influence the measurements. Vibratory and force signals are extracted from the measurements. The following part will consist in explaining the vibratory signals treatment.

Signal processing

The present work reports the development of a new device and a signal processing strategy for studying touch of textured surfaces by friction-induced vibrations. The mechanical stimuli measured during the touch of the surfaces have been enable utilizing Touchy Finger[®]. Since the friction-induced vibrations appear to be among the most meaningful signals in order to perceive and discriminate the fine textures^{17,18,34–36}, the aim is to define a methodology to correctly process the signals measured by our wearable device at the sliding interaction between the fingertip and real surfaces to highlight the perceptible differences.

Signal chopping—To begin with, before analysing any signal, an appropriate pre-processing is required as far as during the measurement, vibrations due to the contact (three distinct patterns) and noise are recorded. There is a need for a pattern of interest recognition as part of the signal processing. Currently, the recognition is carried out with the force signal and a slope detection method which is possible through the setting of a threshold. The calibration threshold is calculated automatically at the end of the 5 measurements for each participant. Calibration of the ring should be done in the following cases: (1) change of user, (2) removal of the ring for the same user. This technique helps identify the specific portions of the vibratory signal that correspond to touch. The signals are saved and the visualization of the force and accelerometer signals allow to adjust this threshold in order to select the interesting portion of the signal without taking into account the noise recorded. Once we have isolated the portions of interest from the signal, we proceed with calculating our parameters. This technic helps identify the vibratory signal parts corresponding to touch.

Parameters of interest—The vibratory level La (dB) values of the vibration accelerations for all cases were calculated to illustrate the influence of the surface roughness on the interface vibration¹⁴. The magnitude of the vibration acceleration signals was found to significantly increase as the roughness was high. Moreover, the vibratory level was calculated for each frequency range depending on each type of mechanoreceptor activation: Merkel's disks (0–5 Hz), Meissner's corpuscles (5–50 Hz), Ruffini's corpuscles (50–300 Hz) and Pacinian corpuscles (300–1000 Hz). The vibratory level can be calculated as shown Eq. (1).

$$La = 20 \log \left(\frac{A_{RMS}}{A_{ref}} \right) \quad (1)$$

Where A_{RMS} is the root mean square value of the acceleration (m/s^2) and A_{ref} the smallest acceleration detected by the sensor ($10^{-6} m/s^2$).

To increase the probability of detecting the differences within the dataset, from the acceleration signal, another parameter is calculated⁸. Depending on the textured surface, a wavelength parameter called λ , frequency dependent, can be calculated for each mechanoreceptor frequency range. The wavelength λ is also a novel calculated parameter resting upon Pr. H. Zahouani's research. It hinges upon the mechanoreceptor, which is assimilable to the dynamic touch acuity.

Static tactile acuity refers to the ability to discern two points of stimulation that are spaced apart on the area of interest on the body. The measurement of spatial tactile acuity is widely practiced and is based on the method developed by E.H. Weber (1996), published in his work on the sense of touch³⁷. The fingertip has the highest tactile acuity of any area of the body, due to its dense innervation by numerous cutaneous mechanoreceptors. The measurement of tactile acuity is typically done in a static manner. For example, at the fingertip, we can discriminate between two points spaced 2 mm apart, while on the back, we can discriminate between two points spaced 50 mm apart³⁸. However, dynamic tactile acuity has not yet been studied in the literature. Dynamic tactile acuity would correspond to the activation of mechanoreceptors during active touch. This could be influenced by the material, texture, or patterns of the surface being characterized. Studying this parameter could help us understand the types of surfaces the finger is sensitive to and how to discriminate them through the excitation of different mechanoreceptors, whose sensitivity varies with different tactile stimulations. It permits to obtain spatial information about what is detected by the corpuscles. In fact, in this pilot study the finger vibrations measurement could provide information about which dimension of the surface roughness can be perceived by each mechanoreceptor.

Our hypothesis is based on the fundamental relationship of vibration dispersion in the different skin layers. This relationship demonstrates that the wavelengths of waves propagating in a dispersive medium depend on the propagation frequency and wave speed, as expressed by relationship (2), with v the velocity (m/s) and f the frequency (Hz):

$$\lambda(f) = \frac{v}{f} \quad (2)$$

This relationship led us to study the wavelengths of the vibration signal in different frequency bands of the signal. We utilized the frequency sensitivity bands of mechanoreceptors as described in the literature. We chose to use these frequency bands as indicators of sensitivity ranges to vibrations: Merkel (0.3–3 Hz) and Meissner (3–50 Hz) are located at the epidermis-dermis junction, while Ruffini (50–300 Hz) and Pacini (300–1000 Hz) are located in the deep dermis and hypodermis, respectively. The expression of the parameter λ , frequency dependent, will be demonstrated through the following steps. First, the accelerometer signal measured during the trials is

$$\gamma(t) = \frac{dv}{dt} \quad (3)$$

In order to process the signal, the Fourier transform of the accelerometer signal, TF is calculated. Its expression can be written as

$$TF[\gamma(t)] = TF\left[\frac{dv}{dt}\right] \quad (4)$$

Consequently, when deriving the Fourier transform TF , the expression can be rewritten as:

$$TF\left[\frac{dv}{dt}\right] = j2\pi f * TF[v(t)] \quad (5)$$

Hence, by utilizing Eq. (2) it is right to write $TF[v(t)] = \lambda(f) f$ and the expression of the Fourier Transform can be written as Eq. (6):

$$TF[\gamma(t)] = TF\left[\frac{dv}{dt}\right] = (j2\pi f) * TF[v(t)] \quad (6)$$

$$= (j2\pi f) * \lambda(f) f = j2\pi f^2 * \lambda(f) \quad (7)$$

Rewriting this expression by using the real part of the complex modulus, the expression become

$$\|TF[\gamma(t)]\| = 2\pi f^2 * \lambda(f) \quad (8)$$

Thus, the wavelengths depend on frequencies through the relationship derived from the Fourier transform, expressed as of $\lambda(f)$ is shown Eq. (9).

$$\lambda(f) = \frac{\|TF[\gamma(t)]\|}{2\pi f^2} \quad (9)$$

This latter relationship comes from the development of the Fourier transform of the acceleration and the taking into account of the dependence of the wavelength on the frequency. This is a fundamental relationship in our study, as within each frequency range of the mechanoreceptors, we observe waves with wavelengths, amplitudes, and frequencies that vary based on the excitation induced by the surface topography, both in terms of amplitude and spatial characteristics. This relationship allows us to make an indirect analogy of the excitation analysis of mechanoreceptors. While it is not a direct measurement of mechanoreceptors, it enables us to study, for each surface relief morphology, the variability of waves perceived in different skin layers.

Plus, to calculate the wavelength of vibrations in each mechanoreceptor, we quantify the centroid frequency Eq. (10). The centroid frequency in each frequency band of Mechanoreceptors is quantified as the center of gravity of the frequencies and has the following expression:

$$f_c = \frac{\sum_{i=1}^N f_i TF(\gamma_i(t))}{\sum_{i=1}^N TF(\gamma_i(t))} \quad (10)$$

The quantitative spectral analysis in each mechanoreceptor is given in Table 3.

The example in Fig. 4 shows the analysis of the vibration signal concerning the touch of abrasive surfaces of different grain sizes ranging from the finest (2400) to the coarsest (320). In this example, the evolution of the wavelengths is shown as a function of the centroid frequencies identified in the Merkel cell frequency band. This example shows how the Merkel cell is solicited by the contact and friction stimulus and provides relevant insight into the methodology used.

Another aspect rarely treated in the analyses of the perception of surfaces concerns the rigidity of the material. The example of Fig. 5 shows for the same texture for two materials of different rigidity, the spectrum of the frequencies of the mechanoreceptors is completely different. This example shows how for rigid surfaces a translation towards high frequencies is operated and how the amplitude in decibels, the wavelength and the centroid frequency are modified in each frequency band of mechanoreceptors. This frequency analysis provides important insight into the stimulation of the mechanoreceptors also depends on the rigidity of the material.

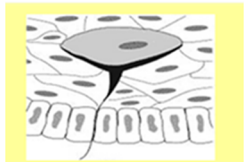
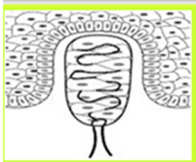

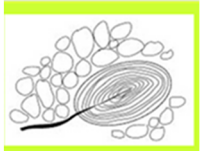
Quantized parameters in the Merkel cell frequency band	Quantized parameters in the Meissner cell frequency band	Quantized parameters in the Ruffini cell frequency band	Quantized parameters in the Pacini cell frequency band
			
$\left[\begin{matrix} La(dB) \\ f_c \rightarrow \lambda(f_c) \end{matrix} \right]_{0;3Hz}^{3Hz}$	$\left[\begin{matrix} La(dB) \\ f_c \rightarrow \lambda(f_c) \end{matrix} \right]_{3Hz}^{50Hz}$	$\left[\begin{matrix} La(dB) \\ f_c \rightarrow \lambda(f_c) \end{matrix} \right]_{50Hz}^{400\ Hz}$	$\left[\begin{matrix} La(dB) \\ f_c \rightarrow \lambda(f_c) \end{matrix} \right]_{400\ Hz}^{1000\ Hz}$

Table 3. Quantitative spectral analysis in each mechanoreceptor frequency range.

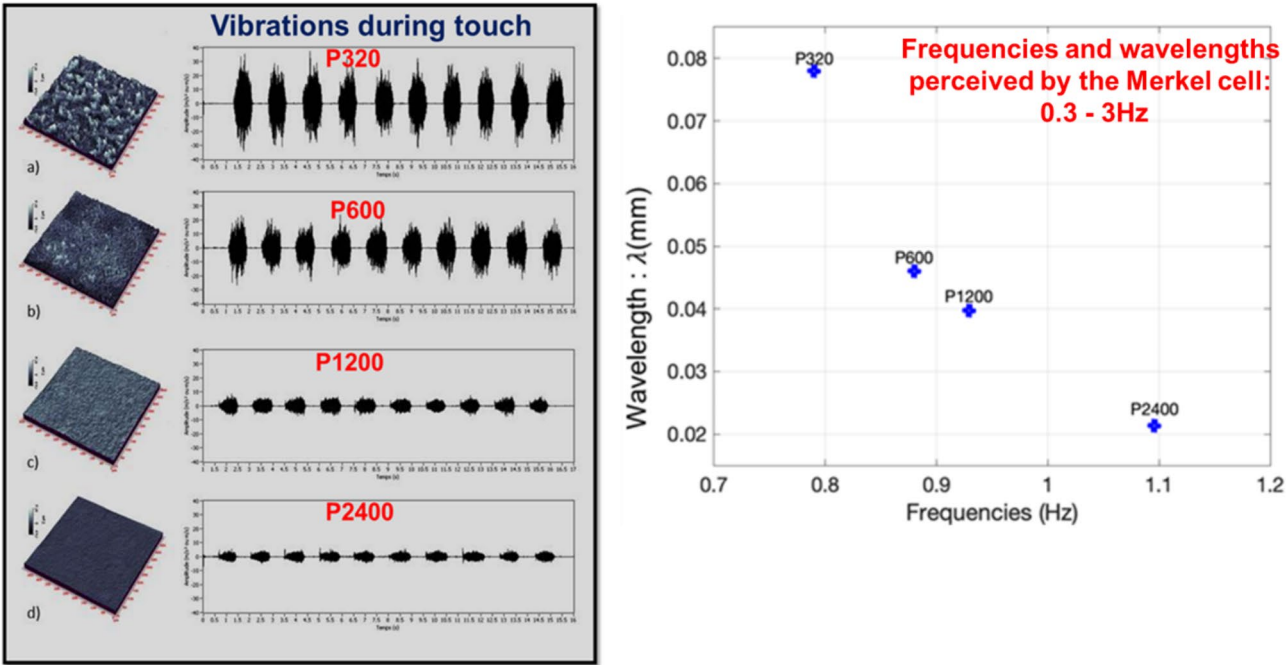


Fig. 4. Analysis of the vibration signal concerning the touch of abrasive surfaces of different grain sizes ranging from the finest (2400) to the coarsest (320).

Power spectral density—The power spectral density (PSD) measurements of the vibration acceleration for the twelve samples were obtained through the analysis in the frequency domain. The fast Fourier transform was utilized to convert the signal from its original time domain to a representation in the frequency domain. All the frequency peaks fell between 0 and 1000 Hz, which corresponds to the range of the perceived frequency of the mechanoreceptors. The dominant and median vibration frequencies and their corresponding magnitude of energy values are noted (see Fig. 6).

Hypotheses

Consequently, to what has been explained, the expectations of the study are to discover interesting correlations between the samples’ topographies and vibrations perceived by the fingerpad. Our principal hypotheses are as follows: (1) skin vibrations measurement can be correlated with the surface topographical characteristics illustrating the reliability of measurements; (2) skin vibrations measured with the Touchy Finger’ device can

Effect of stiffness on spatial-frequency content

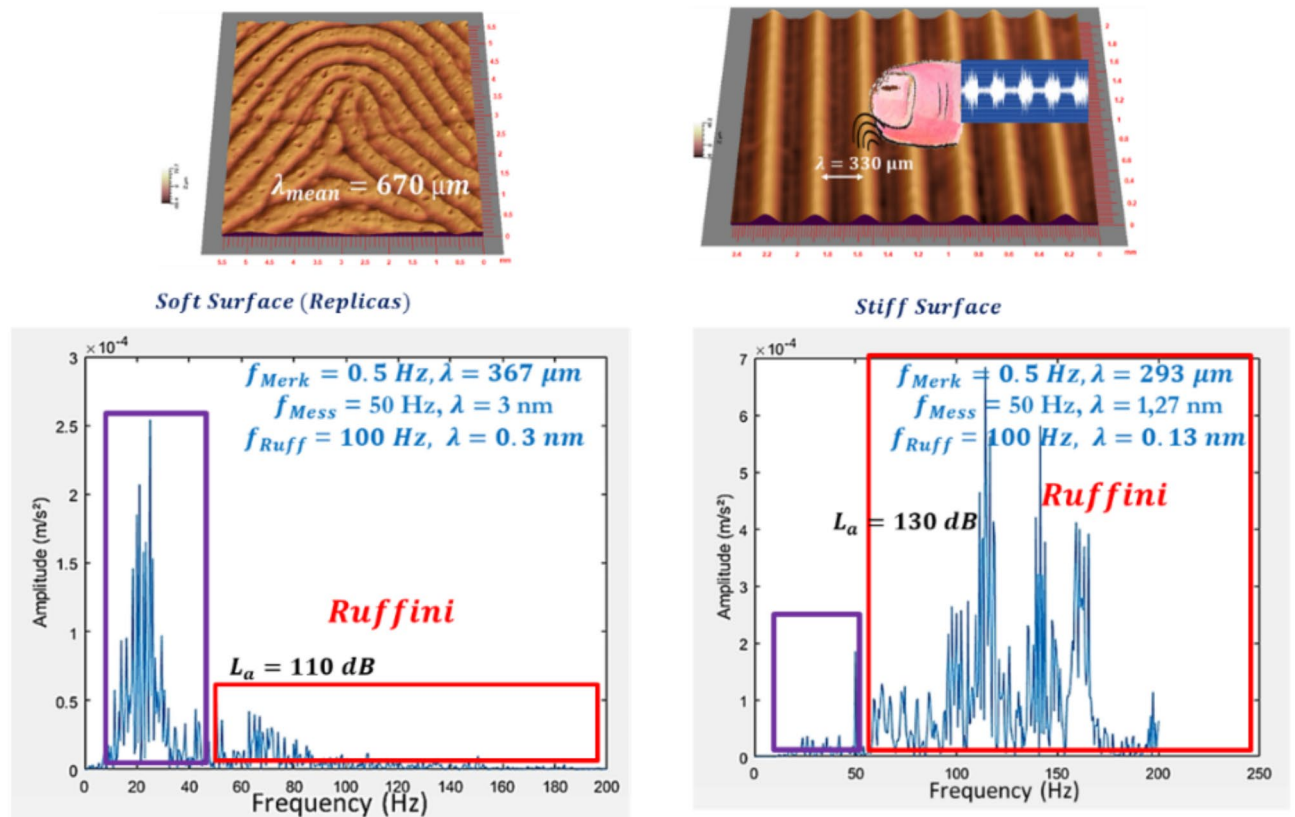


Fig. 5. Effect of stiffness on spatial-frequency content for same surface texture and modification of mechanoreceptor stimulation.

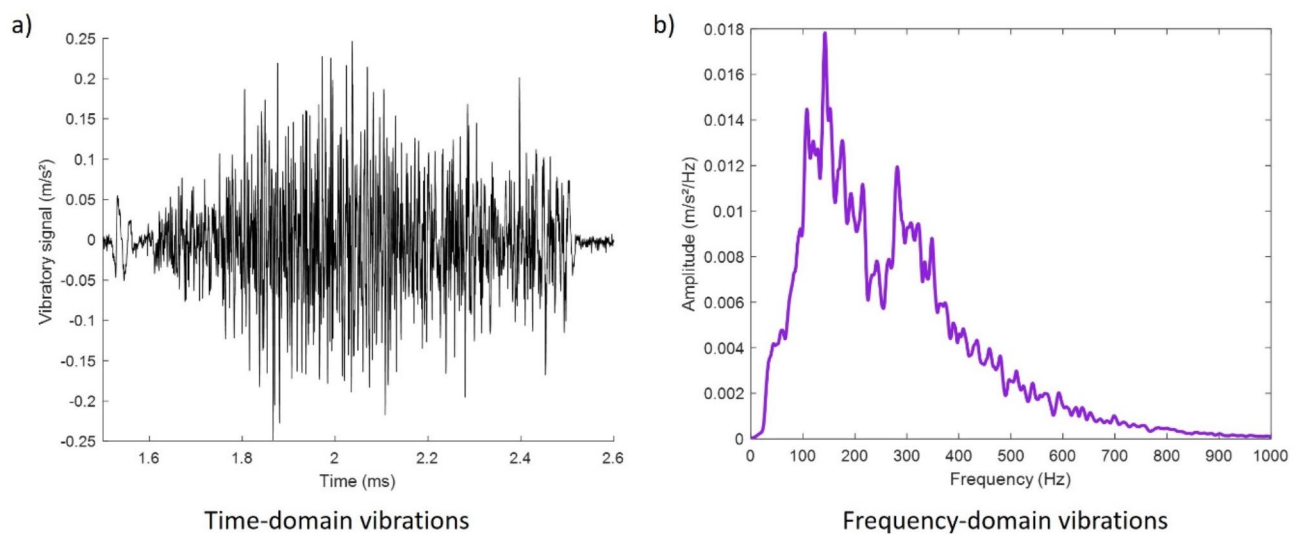


Fig. 6. Vibrations measured with Touchy Finger® during dynamic touch (a) in the time-domain and (b) in the frequency-domain.

discriminate the different samples; (3) skin vibrations measurement can give information about mechanoreceptor's activation on the grounds of signal processing.

Results

This section will focus on the results of the study based on the measurements provided by the device Touchy Finger[®]. In fact, in this work we aim to eliminate the variability introduced by individual perception by relying solely on objective data derived from our measurements: surface roughness and vibration levels. Signal processing, coupled with its connection to mechanoreceptor activation, is expected to provide insights into human perception without the need for training or external influence. The purpose of the Touchy Finger device is to shift the focus away from subjective human perception and center it entirely on the analysis of signals. Furthermore, in our study, we confirmed that the differences between our samples, designed with progressively increasing roughness, are perceptible and easily identifiable by all volunteers. This explains why parameters commonly used in psychophysics, such as JND (Just Noticeable Difference) and PSE (Point of Subjective Equality), which are critical for linking objective measurements to subjective human perception, were not utilized in our research.

Results—power spectral density

The power spectral density (PSD) measurements of the vibration acceleration for different roughness were obtained through the analysis in the frequency domain. The PSD calculation—based on the averages value—and classification are shown in Fig. 7 for all the surfaces of the study. Figure 7 provides the visualization of different surfaces according to the graph shape and peaks. The figure illustrates 3 groups: high roughness (samples 39, 42, 45) from a roughness range from 7.3 μm to 16 μm ; middle roughness (samples 27, 30, 33, 36) from a roughness range from 3.5 μm to 7 μm ; low roughness samples 12, 15, 18, 21, 24) from a roughness range from 0.6 μm to 2.4 μm . It highlights the fact that the PSD, calculated through the vibratory signal, is an interesting visualization tool to classify the surfaces according to their roughness range. For the roughest surface, the dominant vibration frequencies exhibit high energy values. Both values—the maximum amplitude energy and the corresponding frequency—were analysed to see whether these parameters could discriminate the different samples or not. No significant difference was found between the samples when focusing on the high energy value ($p=0.085$ with $\alpha=0.05$) based upon the Kruskal-Wallis test. Nonetheless, a significant difference was ascertained between the samples when focusing on the frequency value depicting the highest energy pick ($p=0.0004$ with $\alpha=0.05$). These results will lead us to focus on the different frequency bands in the following section.

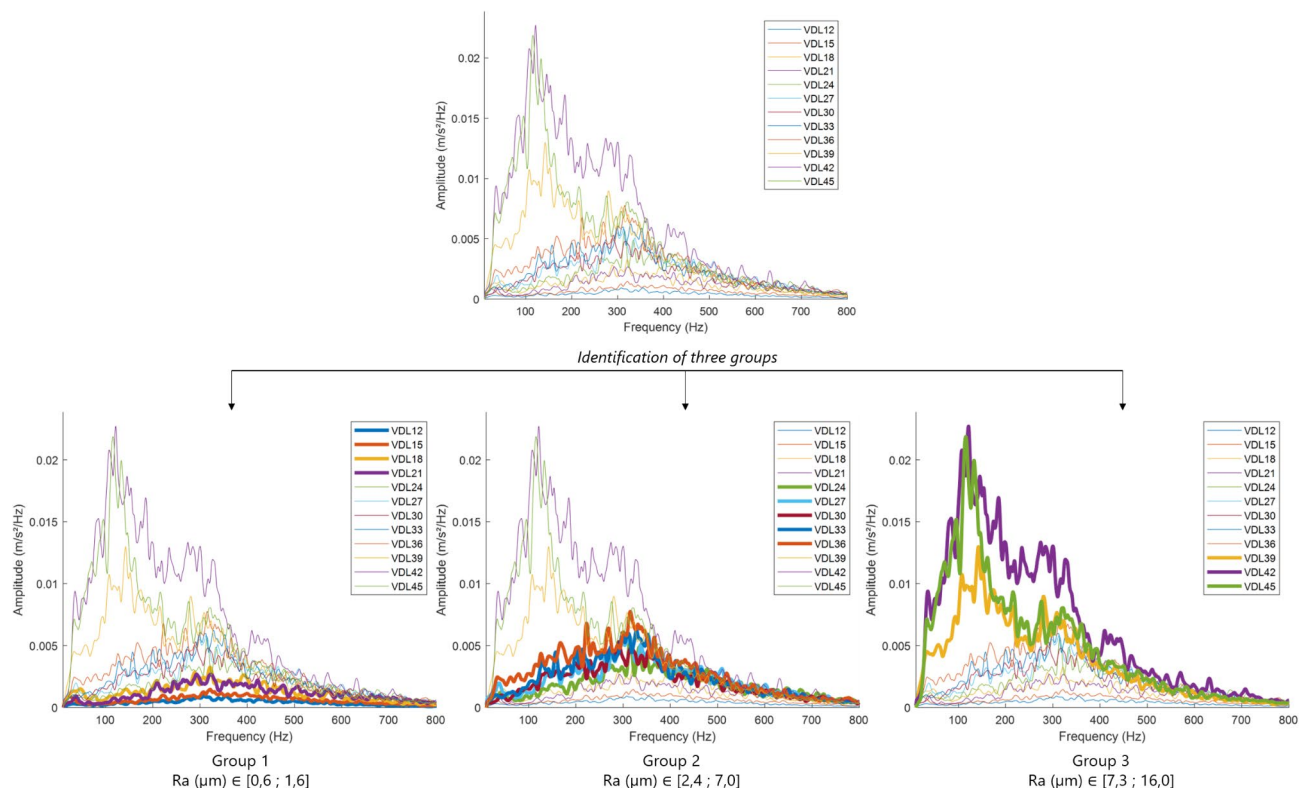


Fig. 7. Power spectral density measurements of the vibration acceleration for the samples and classification of the three sample groups identified.

Samples	<i>La</i> (dB) mean	<i>La</i> (dB) Merkel	<i>La</i> (dB) Meissner	<i>La</i> (dB) Ruffini	<i>La</i> (dB) Pacini
VDL 12	90.3	61.9	61.8	57.8	46.3
VDL 15	90.1	60.1	61.5	57.2	45.1
VDL 18	91.8	61.5	63.8	61.4	50.8
VDL 21	91.4	60.7	64.8	60.1	49.0
VDL 24	92.0	60.2	65.2	61.1	49.5
VDL 27	93.7	60.8	61.3	64.7	56.4
VDL 30	91.8	63.7	60.3	61.8	51.3
VDL 33	93.8	60.7	58.8	65.6	55.9
VDL 36	94.9	61.2	62.5	68.0	58.7
VDL 39	95.3	62.9	65.9	69.9	55.9
VDL 42	96.6	61.9	64.5	72.8	58.4
VDL 45	96.5	62.2	68.2	72.1	57.0

Table 4. Touch parameters extracted from touchy Finger® signals and calculation of the vibratory level for each mechanoreceptor.

$r_{Spearman}$	<i>La</i> (dB) mean	<i>La</i> (dB) Merkel	<i>La</i> (dB) Meissner	<i>La</i> (dB) Ruffini	<i>La</i> (dB) Pacini
Sa (mm)	0.82	-0.13	0.43	0.83	0.75
Sq (mm)	0.82	-0.13	0.43	0.84	0.76
SPt (mm)	0.82	-0.15	0.43	0.83	0.74
Sz (mm)	0.81	-0.14	0.43	0.83	0.74
Spm (mm)	0.78	-0.09	0.44	0.79	0.68
Svm (mm)	0.85	-0.15	0.45	0.86	0.79
Smx (mm)	0.91	-0.35	0.58	0.92	0.83
Smy (mm)	0.86	-0.22	0.52	0.88	0.77

Table 5. Spearman correlation table between topographical parameters and vibration level.

Results—vibratory level analysis

Table 4 illustrates the results of the vibratory level values. For each sample are calculated the mean value considering the data collected from the ten participants. To begin with, the aim was to ascertain a correlation between the vibratory level measurement and topographical data extracted from the twelve samples. For the samples with low roughness, the vibratory level value is close to 90 dB (samples 12 and 15), while for rougher surfaces the vibratory level value is close to 97 dB (samples 42 and 45). Comparing the opposite samples, 7 dB is a consequent gap. In addition, to ensure that this vibratory parameter can be relevant, a statistical analysis was performed to identify whether the measurement of the vibratory level can discriminate the different samples with this low range of roughness variation. The Kruskal-Wallis test is a non-parametric, it has been employed to evaluate our 12 independent samples about the vibratory level value. According to the statistical results, a significant difference of *La* (dB) depending on the samples has been ascertained (p-value < 0.0001 with $\alpha = 0.05$). This input highlights the fact that these vibratory signals from the finger's skin measurement can provide reliable information and can discriminate the surfaces.

Then, the correlation between the parameters was studied. The Spearman coefficient evaluates the monotonic relationship between variables, meaning it can capture relationships that are not necessarily linear but follow an increasing or decreasing trend. This test provides a correlation coefficient $r_{Spearman}$, which is the Spearman coefficient.

The Spearman coefficient was investigated to show the relations between topographical parameters and the vibration level *La* (dB). Results summarized in Table 5 show high correlations between *La* (dB) mean and the roughness parameters. Figure 8a and b depict the significant correlation between the 3D roughness amplitude

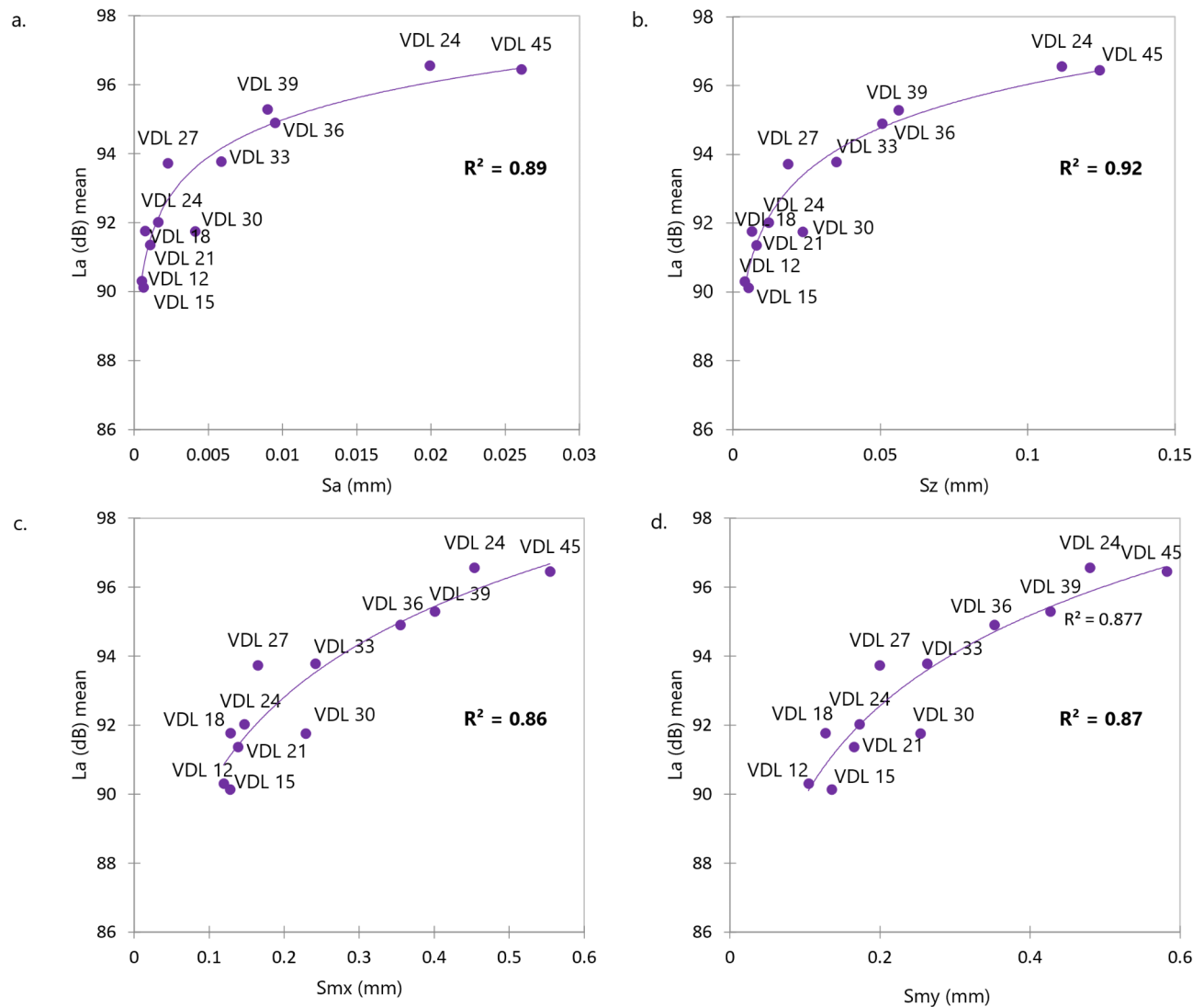


Fig. 8. (a) Graphical correlation between the vibratory level La (dB) mean and amplitude parameter Sa (mm). (b) Graphical correlation between the vibratory level La (dB) mean and amplitude parameter Sz (mm). (c) Graphical correlation between the vibratory level La (dB) mean and spacing parameter Smx (mm). (d) Graphical correlation between the vibratory level La (dB) and spacing parameter Smy (mm).

parameters— Sa (mm) and Sz (mm)—and the mean vibratory level calculated for each surface. The logarithmic correlation ($R^2 = 0.89$) highlights the fact that the rougher the surface is, the more the vibrations are amplified within the finger, showing the influence of the fingerprints¹⁴. It underlines a correlation between the vibratory level and the amplitude parameter of the surface. Plus, Fig. 8c and d illustrates the significant correlation between the parameters Smx (mm), Smy (mm) and the mean vibratory level calculated for each surface. The linear correlation ($R^2 = 0.86$ and $R^2 = 0.87$, respectively) emphasizes the fact the rougher the surface is, the more the patterns are spaced and trigger the skin by increasing the vibrations. It delivers a correlation between the vibratory level and the spacing parameter of the surface.

Moreover, results show better correlations for the vibratory level calculated on the frequency range of mechanoreceptors Ruffini and Pacini. The results summarized in Table 5 show high correlations between La (dB) Ruffini, La (dB) Pacini and the roughness parameters. Figure 9 depicts the significant correlation between the 3D roughness Smx (mm) and Smy (mm). In contrast to the results for other mechanoreceptors, Merkel and Meissner, the values of the Spearman coefficient ($r_{Spearman} < 0.6$) indicate no noteworthy correlation. This underscores that for these textured surfaces, information gathered on frequencies between 50 and 1000 Hz, corresponding to the Ruffini and Pacini frequency bands, is the most reliable for discriminating the samples. Particularly within the Ruffini frequency band (50–300 Hz), with $r_{Spearman} > 0.83$.

The statistical analysis confirmed these observations, revealing a significant difference between the samples when focusing on La (dB) Ruffini (p-value < 0.0001 with $\alpha = 0.05$) and La (dB) Pacini (p-value < 0.0001 with $\alpha = 0.05$). Conversely, there is no significant difference between the samples when focusing on La (dB) Merkel (p-value = 0.58 with $\alpha = 0.05$) and La (dB) Meissner (p-value = 0.08 with $\alpha = 0.05$).

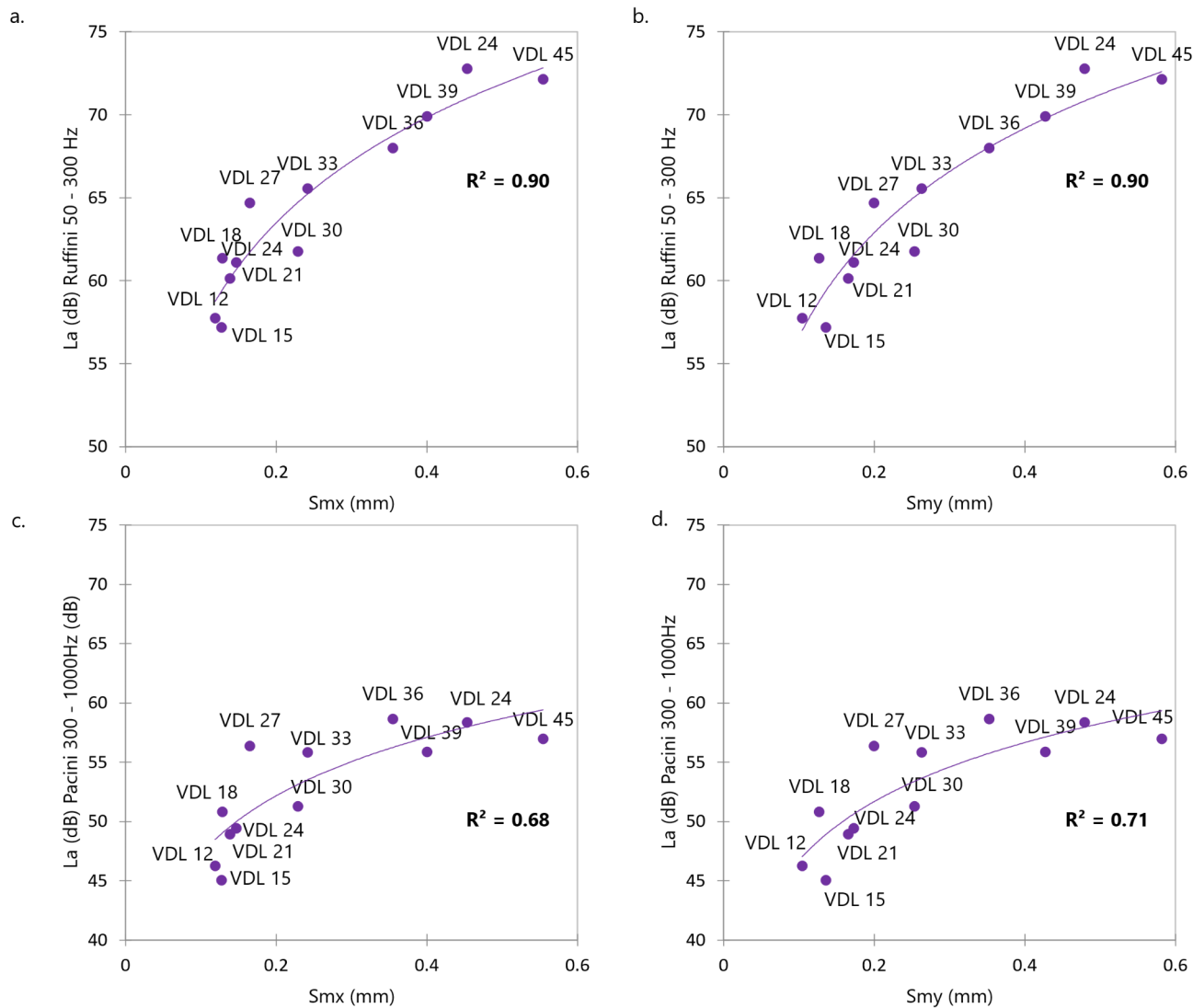


Fig. 9. (a) Graphical correlation between the vibratory level La (dB) Ruffini and spacing parameter Smx (mm). (b) Graphical correlation between the vibratory level La (dB) Ruffini and spacing parameter Smy (mm). (c) Graphical correlation between the vibratory level La (dB) Pacini and spacing parameter Smx (mm). (d) Graphical correlation between the vibratory level La (dB) Pacini and spacing parameter Smy (mm).

These outcomes validate the consistency of the measurements acquired with the augmented finger developed to measure the skin vibrations while rubbing a textured surface. An interesting correlation was found between the vibratory level value and topographical parameters being contingent upon the amplitude and spacing parameters of the surface, comparable to the results of Massimiani et al.^{26,28}. Thus, it validated our hypotheses 1 and 2.

Results—wavelength analysis

The Spearman coefficient was investigated to show the relations between topographical parameters and the parameter λ (mm). Results summarized in Tables 6 and 7, indicate medium correlations between the wavelength and the roughness parameters. Low correlations were observed with λ Meissner ($r_{Spearman} < 0.36$) and with λ Merkel ($r_{Spearman} < -0.39$). Notably, the most significant correlations with the roughness parameters were observed when comparing them with λ Pacini ($r_{Spearman} > 0.54$) and λ Ruffini ($r_{Spearman} > 0.59$). Moreover, positive trends suggest that as the parameter increases, the wavelength also increases. The trend observed according to the mechanoreceptors follow the same results as those of the vibratory level.

In fact, these medium to high correlations can be interpreted as an indicator of the ability of information derived from vibratory signals to detect what the human finger perceives during measurements: the texture and how it stimulates our various cutaneous mechanoreceptors. The results from the previous tables indicate that different surface characteristics have varying influences on mechanoreceptors. Certain surface parameters show a strong correlation with the vibratory responses of mechanoreceptors, which may be due to their frequency sensitivity range and how the surface texture interacts with the fingertip. Correlation results are shown Fig. 10.

Samples	λ (mm) Merkel	λ (mm) Meissner	λ (mm) Ruffini	λ (mm) Pacini
VDL 12	5.46 E-02	1.80 E-03	3.15 E-05	8.30 E-07
VDL 15	6.48 E-02	1.37 E-03	3.02 E-05	6.55 E-07
VDL 18	5.33 E-02	1.49 E-03	3.54 E-05	8.68 E-07
VDL 21	5.05 E-02	1.42 E-03	3.61 E-05	7.59 E-07
VDL 24	5.20 E-02	1.37 E-03	4.11 E-05	7.35 E-07
VDL 27	2.67 E-02	2.07 E-03	4.23 E-05	1.41 E-06
VDL 30	4.78 E-02	1.31 E-03	3.20 E-05	9.20 E-07
VDL 33	3.94 E-02	1.55 E-03	3.15 E-05	1.20 E-06
VDL 36	2.81 E-02	1.68 E-03	4.02 E-05	1.59 E-06
VDL 39	5.01 E-02	1.87 E-03	4.44 E-05	1.21 E-06
VDL 42	3.01 E-02	1.84 E-03	4.56 E-05	1.50 E-06
VDL 45	5.67 E-02	1.87 E-03	4.76 E-05	1.25 E-06

Table 6. Touch parameters extracted from touchy Finger® signals and calculation of the wavelength for each mechanoreceptor.

$r_{Spearman}$	λ (mm) Merkel	λ (mm) Meissner	λ (mm) Ruffini	λ (mm) Pacini
Sa (mm)	-0.47	0.32	0.56	0.66
Sq (mm)	-0.48	0.33	0.57	0.67
SPt (mm)	-0.47	0.34	0.54	0.65
Sz (mm)	-0.46	0.36	0.54	0.65
Spm (mm)	-0.39	0.35	0.49	0.59
Svm (mm)	-0.50	0.34	0.61	0.70
Smx (mm)	-0.49	0.24	0.66	0.77
Smy (mm)	-0.48	0.32	0.62	0.70

Table 7. Spearman correlation table between topographical parameters and wavelength.

Interpretations specific to each mechanoreceptor response will be delved. Merkel Discs are sensitive to continuous pressure and fine textures. Negative correlations might indicate that certain smooth or less pronounced textures reduce the activation of Merkel receptors, meaning these receptors are less stimulated by surfaces that do not produce sustained skin deformation. Meissner Corpuscles are sensitive to low-frequency changes in texture and pressure. Moderate correlations suggest that surface textures interact with these mechanoreceptors, but the activation is neither as direct nor as pronounced as with Ruffini or Pacinian receptors. This could be the case for textures that produce more subtle changes in the vibrations or pressures perceived by the finger. And according to the literature, we know that Ruffini and Pacini receptors are the most widespread within the fingertip. Ruffini endings are sensitive to skin stretch and slow deformations. High correlations with these values suggest that surface characteristics cause noticeable skin deformations, which are well detected by these mechanoreceptors through the study of vibratory signals. This may be due to coarser textures or surface patterns

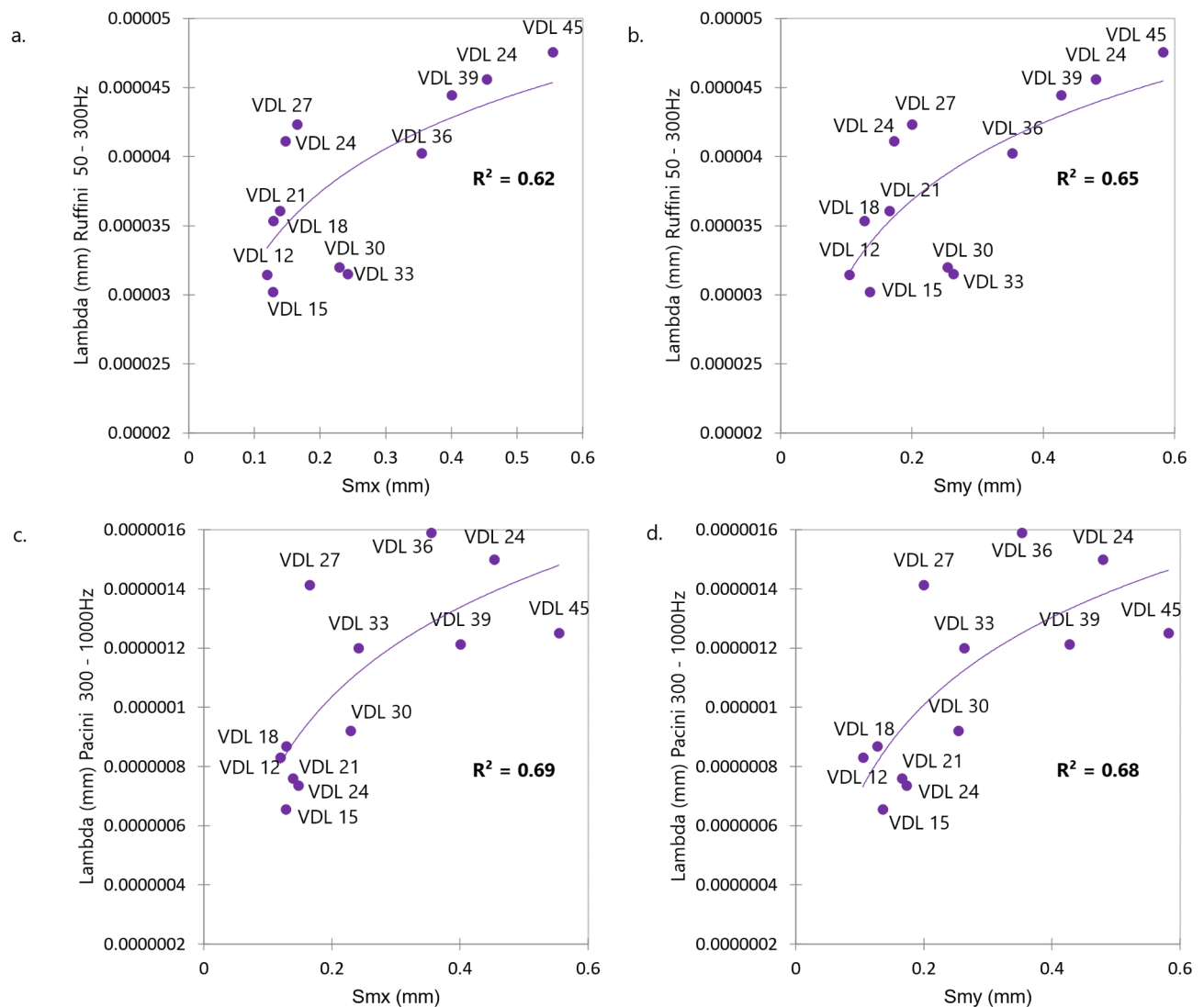


Fig. 10. (a) Graphical correlation between the λ Ruffini and spacing parameter Smx (mm). (b) Graphical correlation between the vibratory level λ Ruffini and spacing parameter Smy (mm). (c) Graphical correlation between the vibratory level λ Pacini and spacing parameter Smx (mm). (d) Graphical correlation between the vibratory level λ Pacini and spacing parameter Smy (mm).

that result in significant changes in skin pressure or tension during movement. Pacinian Corpuscles are highly sensitive to rapid vibrations and pressure changes. Strong correlations with Pacinian responses indicate that the textures generate high-frequency vibrations that stimulate these mechanoreceptors. These textures may include micro-asperities or repetitive patterns that, when swept by the finger, produce high-frequency vibrations.

Discussion

Although the investigation bespoke promising research advancements and equivalent promising results were found on another set of samples, several limitations were encountered. To begin with, the tests have been performed on ten participants, measurements have been repeated numerous, and yet including more participants and different age groups can solidify the global output. Moreover, the gender effect, which may lead to different vibratory responses due to tribological and dynamical properties, was not addressed in this paper. The distribution of mechanoreceptors—corresponding to fingerpad and gender—during touch, which also play a role in tactile perception, was not examined¹⁴. Notwithstanding, investigating the gender effect ought to be of future interest. Furthermore, this research focused on the roughness of a polymer-based surface, therefore, different materials ought to be sifted through so as to assess the skin deformation. Other limitations include the in-situ control of skin hydration, the measurement of skin mechanical properties, and the development of mathematic models that link vibration as a function of surface features, velocity, and so on. Consequently, all these considerations are of utmost importance to unveil the underlying mechanism of finger perception from tribological and dynamical perspectives.

Conclusion

The innovation of this study lies in the use of a new tribohaptic device, which allows the fingertip to be completely exposed and ensures the hand's movement remains unrestricted. Additionally, the novelty extends to a new approach for processing vibratory signals by frequency bands, enabling a direct link between tactile stimuli and the activation of cutaneous mechanoreceptors. While hypotheses 1 and 2 may seem self-evident, they were essential to verify in order to ensure the reliability of the measurements obtained with this device. By confirming these hypotheses, we can confidently analyze the data and rely on the signal processing method to provide accurate insights into what the fingertip perceives.

An innovative wearable haptic device capable of measuring the interaction between the finger and the surface was introduced. Onboard sensors enable skin vibration measurement, which makes the technology advantageously portable and easily usable. The device was conceived to record acceleration signals from the finger touching a textured surface, therefore the processing of these signals could provide essential parameters to correlate subjective data from the surface roughness perception to objective data collected by physical measurement and signal processing. In this research, the objective was to discover a specific correlation between touch perception and objective parameters. Tools such as neural networks would make it possible to deepen the study and examine other parameters of discrimination. Yet in future investigations, it could be of great interest to scour the aging effect on these measurements as tactile perception declines with age. For industrial purpose, the device could provide paramount comprehension of everyday interactions.

Data availability

All data generated or analysed during this study are included in this published article and its supplementary information files.

Received: 4 July 2024; Accepted: 27 February 2025

Published online: 22 March 2025

References

1. Lederman, S. J. Tactual roughness perception: spatial and temporal determinants. *Can. J. Psychol.* **37**, 498–511. <https://doi.org/10.1037/h0080750> (1983).
2. Katz, D. The world of touch. *Psychol. Press. eBooks* <https://doi.org/10.4324/9780203771976> (2013).
3. Weber, A. I. et al. Spatial and temporal codes mediate the tactile perception of natural textures. *Proc. Natl. Acad. Sci. U.S.A.* **110**, 17107–17112. <https://doi.org/10.1073/pnas.1305509110> (2013).
4. Manfredi, L. R. et al. Natural scenes in tactile texture. *J. Neurophysiol.* **111**, 1792–1802. <https://doi.org/10.1152/jn.00680.2013> (2014).
5. Lederman, S. J. & Klatzky, R. L. Hand movements: a window into haptic object recognition. *Cogn. Psychol.* **19**, 342–368. [https://doi.org/10.1016/0010-0285\(87\)90008-9](https://doi.org/10.1016/0010-0285(87)90008-9) (1987).
6. McGrath, J. A. & Uitto, J. *Anatomy and Organization of Human Skin. Rook's Textbook of Dermatology* (Wiley eBooks, 2010). <https://doi.org/10.1002/9781444317633>.
7. Manfredi, L. R. et al. The effect of surface wave propagation on neural responses to vibration in primate glabrous skin. *PLoS One* **7**, e31203. <https://doi.org/10.1371/journal.pone.0031203> (2012).
8. Delhay, B., Hayward, V., Lefèvre, P. & Thonnard, J. L. Texture-induced vibrations in the forearm during tactile exploration. *Front. Behav. Neurosci.* **6**, 85. <https://doi.org/10.3389/fnbeh.2012.00037> (2012).
9. Bolanowski, S. J., Gescheider, G. A., Verrillo, R. T. & Checkosky, C. M. Four channels mediate the mechanical aspects of touch. *J. Acoust. Soc. Am.* **84**, 1680–1694. <https://doi.org/10.1121/1.397184> (1988).
10. Blake, D. T., Hsiao, S. S. & Johnson, K. O. Neural coding mechanisms in tactile pattern recognition: the relative contributions of slowly and rapidly adapting mechanoreceptors to perceived roughness. *J. Neurosci.* **17**, 7480–7489. <https://doi.org/10.1523/jneurosci.17-19-07480.1997> (1997).
11. Bolanowski, S. J. & Zwillocki, J. J. Intensity and frequency characteristics of Pacinian corpuscles. I. Action potentials. *J. Neurophysiol.* **51**, 793–811. <https://doi.org/10.1152/jn.1984.51.4.793> (1984).
12. Cascio, C. J. & Sathian, K. Temporal cues contribute to tactile perception of roughness. *Journal Neurosci.* **21**, 5289–5296. <https://doi.org/10.1523/JNEUROSCI.21-14-05289.2001> (2001).
13. Skedung, L. et al. Feeling small: exploring the tactile perception limits. *Sci. Rep.* **3**, 89. <https://doi.org/10.1038/srep02617> (2013).
14. Abdouni, A., Vargiolu, R. & Zahouani, H. Impact of finger biophysical properties on touch gestures and tactile perception: aging and gender effects. *Sci. Rep.* **8**, 85. <https://doi.org/10.1038/s41598-018-30677-2> (2018).
15. Orr, A. W., Helmke, B. P., Blackman, B. R. & Schwartz, M. A. Mechanisms of mechanotransduction. *Dev. Cell.* **10**, 11–20. <https://doi.org/10.1016/j.devcel.2005.12.006> (2006).
16. Cardozo, C. P. *Mechanotransduction: Overview* 217 (Elsevier eBooks, 2020). <https://doi.org/10.1016/b978-0-12-801238-3.62233-x>.
17. Zahouani, H., Mezghani, S., Vargiolu, R., Hoc, T. & Mansori, M. E. Effect of roughness on vibration of human finger during a friction test. *Wear* **301**, 343–352. <https://doi.org/10.1016/j.wear.2012.11.028> (2013).
18. Amaied, E., Vargiolu, R., Bergheau, J. M. & Zahouani, H. Aging effect on tactile perception: experimental and modelling studies. *Wear* **332–333**, 715–724. <https://doi.org/10.1016/j.wear.2015.02.030> (2015).
19. Derler, S., Schrade, U. & Gerhardt, L. -C. Tribology of human skin and mechanical skin equivalents in contact with textiles. *Wear* **263**, 1112–1116. <https://doi.org/10.1016/j.wear.2006.11.031> (2007).
20. Derler, S., Gerhardt, L., Lenz, A., Bertaux, E. & Hadad, M. Friction of human skin against smooth and rough glass as a function of the contact pressure. *Tribol. Int.* **42**, 1565–1574. <https://doi.org/10.1016/j.triboint.2008.11.009> (2009).
21. Dzidek, B. M., Adams, M. J., Andrews, J. W., Zhang, Z. & Johnson, S. A. Contact mechanics of the human finger pad under compressive loads. *J. R. Soc. Interface* **14**, 20160935. <https://doi.org/10.1098/rsif.2016.0935> (2017).
22. Sirin, O., Barrea, A., Lefèvre, P., Thonnard, J. L. & Basdogan, C. Fingerprint contact evolution under electrovibration. *J. R. Soc. Interface* **16**, 20190166. <https://doi.org/10.1098/rsif.2019.0166> (2019).
23. Adams, M. J. et al. Finger pad friction and its role in grip and touch. *J. Royal Soc. Interface* **10**, 20120467. <https://doi.org/10.1098/rsif.2012.0467> (2013).
24. Ndengue, J. D. et al. Tactile perception and friction-induced vibrations: discrimination of similarly patterned Wood-Like surfaces. *IEEE Trans. Haptics* **10**, 409–417. <https://doi.org/10.1109/TOH.2016.2643662> (2017).
25. Fagiani, R., Massi, F., Chatelet, E., Costes, J. P. & Berthier, Y. Contact of a finger on rigid surfaces and textiles: friction coefficient and induced vibrations. *Tribol. Lett.* **48**, 145–158. <https://doi.org/10.1007/s11249-012-0010-0> (2012).

26. Massi, F., Vittecoq, E., Chatelet, E., Saulot, A. & Berthier, Y. Design of a tribometer for investigating tactile perception. *Proc. Inst. Mech. Eng. Part. J. J. Eng. Tribol.* **232**, 773–784. <https://doi.org/10.1177/1350650113518906> (2014).
27. Ding, S., Pan, Y., Tong, M. & Zhao, X. Tactile perception of roughness and hardness to discriminate materials by Friction-Induced vibration. *Sensors* **17**, 2748. <https://doi.org/10.3390/s17122748> (2017).
28. Felicetti, L., Chatelet, E., Latour, A., Cornuault, P. H. & Massi, F. Tactile rendering of textures by an electro-active polymer piezoelectric device: mimicking friction-Induced vibrations. *Biotribology* **31**, 100211. <https://doi.org/10.1016/j.biotri.2022.100211> (2022).
29. Beebe, D. J., Denton, D. D., Radwin, R. G. & Webster, J. G. A silicon-based tactile sensor for finger-mounted applications. *IEEE Trans. Bio-med. Eng.* **45**, 151–159. <https://doi.org/10.1109/10.661263> (1998).
30. Kikuuwe, R., Nakamura, K. & Yamamoto, M. Finger-Mounted tactile sensor for evaluating surfaces. *J. Robot. Mechatron.* **24**, 430–440. <https://doi.org/10.20965/jrm.2012.p0430> (2012).
31. Assaf, T., Roke, C., Rossiter, J., Pipe, T. & Melhuish, C. Seeing by touch: evaluation of a soft biologically-Inspired artificial fingertip in Real-Time active touch. *Sensors* **14**, 2561–2577. <https://doi.org/10.3390/s140202561> (2014).
32. Oddo, C. M., Controzzi, M., Beccai, L., Cipriani, C. & Carrozza, M. C. Roughness encoding for discrimination of surfaces in artificial active-touch. *IEEE Trans. Robot.* **27**, 522–533. <https://doi.org/10.1109/TRO.2011.2116930> (2011).
33. Zhou, X. et al. Effect of finger sliding direction on tactile perception, friction and dynamics. *Tribol. Lett./Tribol. Lett.* **68**, 859 <https://doi.org/10.1007/s11249-020-01325-6> (2020).
34. Thieulin, C., Pailler-Mattei, C., Vargiolu, R., Lancelot, S. & Zahouani, H. Study of the tactile perception of bathroom tissues: comparison between the sensory evaluation by a handfeel panel and a tribo-acoustic artificial finger. *Colloids. Surf. B. Biointerfaces.* **150**, 417–425. <https://doi.org/10.1016/j.colsurfb.2016.11.006> (2017).
35. Cornuault, P. H., Carpentier, L., Bueno, M. A., Cote, J. M. & Monteil, G. Influence of physico-chemical, mechanical and morphological fingerpad properties on the frictional distinction of sticky/slippery surfaces. *J. Royal Soc. Interface* **12**, 20150495. <https://doi.org/10.1098/rsif.2015.0495> (2015).
36. Massimiani, V. et al. The role of mechanical stimuli on hedonistic and topographical discrimination of textures. *Tribol. Int.* **143**, 106082. <https://doi.org/10.1016/j.triboint.2019.106082> (2020).
37. Weber, E. H. E. H. *Weber on the Tactile Senses* 2nd edn (eds Ross, H. E. & Murray, D. J.) (Taylor & Francis, 1996).
38. Tong, J., Mao, O. & Goldreich, D. Two-Point orientation discrimination versus the traditional Two-Point test for tactile Spatial acuity assessment. *Front. Hum. Neurosci.* **7**, 58. <https://doi.org/10.3389/fnhum.2013.00579> (2013).

Acknowledgements

The authors acknowledge with thanks Laboratoire de Tribologie et Dynamique des Systèmes (LTDS) for hosting the research project and Renault Group for funding this project.

Author contributions

R.S. conceived the experiments with the assistance of R.V. and H.Z.; R.S. conducted the experiments and analysed the results; R.S. wrote the main manuscript text and prepared the figures with the assistance of H.Z. All authors reviewed the manuscript.

Funding

The authors acknowledge the financial support provided by Renault Group.

Competing interests

The authors declare no competing interests.

Informed consent

Informed consent was obtained from all the participants of the study.

Additional information

Supplementary Information The online version contains supplementary material available at <https://doi.org/10.1038/s41598-025-92379-w>.

Correspondence and requests for materials should be addressed to R.S.

Reprints and permissions information is available at www.nature.com/reprints.

Publisher's note Springer Nature remains neutral with regard to jurisdictional claims in published maps and institutional affiliations.

Open Access This article is licensed under a Creative Commons Attribution-NonCommercial-NoDerivatives 4.0 International License, which permits any non-commercial use, sharing, distribution and reproduction in any medium or format, as long as you give appropriate credit to the original author(s) and the source, provide a link to the Creative Commons licence, and indicate if you modified the licensed material. You do not have permission under this licence to share adapted material derived from this article or parts of it. The images or other third party material in this article are included in the article's Creative Commons licence, unless indicated otherwise in a credit line to the material. If material is not included in the article's Creative Commons licence and your intended use is not permitted by statutory regulation or exceeds the permitted use, you will need to obtain permission directly from the copyright holder. To view a copy of this licence, visit <http://creativecommons.org/licenses/by-nc-nd/4.0/>.

© The Author(s) 2025